Fachtagung "Experimentelle Strömungsmechanik"
3. – 5. September 2019, Erlangen

Experimental characterization of a bubble column reactor operated under the influence of enforced pulsation

Experimentelle Charakterisierung eines Blasensäulenreaktors unter Einwirkung erzwungener Pulsationen

Christoph Gerstenberg[1], Christopher McHardy[1], Deborah Becker[1], Bastian Eysel[1], Giovanni Luzi[2], Cornelia Rauh[1,2]
[1] Technische Universität Berlin, Fachgebiet Lebensmittelbiotechnologie und -prozesstechnik, Königin-Luise Straße 22, 14195 Berlin
[2] LSTME Busan Branch, Busan 46742, Republic of Korea

Bubble column reactors, enforced pulsation, gas hold-up, bubble break-up, bubble size
Blasensäulenreaktoren, erzwungene Pulsation, Gasgehalt, Blasenaufbruch, Blasengröße

Abstract

Bubble column reactor's versatility makes them a common unity of operation in (bio)-chemical processes. To quantify a reactor's efficiency, characteristic parameters such as gas hold-up, bubble size, bubble generating frequency, and mass transfer coefficient are utilized, which are closely link to the reactor's configurations and the resulting flow conditions.
In this work, a laboratory scale bubble column reactor is characterized with the previously specified parameters. Furthermore, the influence of forced pulsation of the gas and liquid phase on the operating parameters is studied. Reportedly, forced pulsations can improve the reactor's performance. The gas phase is oscillated with a fluidic oscillator and its effect on the bubble size and bubble formation is examined. In a second experiment, the impact of a pulsation of the liquid phase with a high precision linear motor is investigated.
Results show that the pulsation of the liquid phase significantly increases the gas hold-up, which is dependent on both the pulsation frequency and amplitude. High-speed recordings revealed that the pulsation mainly affects the bubble generation, while under specific circumstances the flow conditions and bubble break-up can be positively influenced.

Introduction

Improving the performance of bubble column reactors is the subject of numerous research and development projects. The efficiency of a bubble column reactor can be quantified by characteristic parameters such as gas hold-up, bubble size, bubble generating frequency, mass transfer coefficient, power consumption, product yields, and others. It has been reported that forced pulsation of either liquid or gas phase has a positive effect on operating parameters and flow conditions (Brittle et al., 2015, Krishna and Ellenberger 2002).
With an oscillation of the gas phase, mono-dispersed microbubble clouds can be produced that increase gas hold-up and mass transfer rate (up to 29 %) (Al-Mashhadani et al., 2011). An advantageous by product of microbubbles is that mixing efficiency as well as bubble residence time are increased (Al-Mashhadani et al., 2015). Furthermore, it has been reported, that at an optimal oscillation frequency, the average diameter of single bubble can be reduced by 15% compared to bubbles created without an oscillation of the gas phase (Brittle et al., 2015). This phenomenon was contributed to a premature detachment of the bubble from the nozzle due to an additional lift force associated with the momentum of the gas flow entering the bubble. Additionally, forced pulsation of the gas phase requires low initial costs and is simple to

GALA e.V., Karlsruhe, Germany, ISBN 978-3-9816764-6-4

implement to pre-existing setups, which makes it a promising subject of research (Vaclav Tesar et al. 2006).
Forced pulsation of the liquid phase is also capable of increasing mass transfer rates. Different theories have been presented that try to explain the enhanced mass transfer rate. An increase in interfacial area per unit volume associated with an increase in gas hold-up at specific resonance frequencies has been proposed (Harbaum and Houghton, 1962). Others suggested that an increase in mass transfer rate is not solely due to an increase in interfacial area, but caused by an increase in turbulence, which improves mass transfer (Krishna and Ellenberger, 2002). Others have argued that the pulsation of the liquid phase causes shear forces, which itself causes the bubble boundary layer to detach. This prevents the build-up of boundary layer that are highly saturated with gas around small bubbles (Baird and Davidson, 1962). Furthermore, it has been shown that vibrations help maintain the homogeneous flow regime by producing bubbles with smaller diameters with most of the bubbles being disintegrated, while still inside the sparger or shortly after exiting the orifice either by shear stress or turbulence (Waghmare et al., 2007, Ellenberger et al., 2003).
This work aims to study the effect the combination of force pulsation of the liquid and gas has on the bubble size and frequency, bubble generation process, and bubble break-up.

Material and Methods

Experimental setup for the oscillation of gas phase

A bubble column reactor (PMMA, $d_i = 7\ \mathrm{cm}$, $\mathrm{h} = 42\ \mathrm{cm}$), is mounted on a pedestal (height of 19 cm) and placed in an aquarium (not shown) filled with distilled water to a height of 42 cm, cf. Figure 1, left. Two dip tube spargers ($d_o = 2\ mm$) and two half ring spargers with eight holes ($d_o = 0.9\ mm$) are studied. A self-excited, non-mechanical fluidic oscillator alternates the air flow between two outlets at a specific frequency that can be changed with an adjustable feedback loop (Václav Tesař, et al. 2006). Experiments were performed at gas flow rates of 0.1 L/min, 0.4 L/min, 0.7 L/min to 1.0 L/min per sparger. As a significantly higher input gas flow rate is required for maintaining the bistable condition of the fluidic oscillator, bleed valves vent the excess air while throttle valves in conjunction with pressure gauges and a flow meter control the air flow throughout the entire experiment.

Experimental setup for the vibration of liquid phase

The air flow is first roughly regulated with a pressure regulator then fine-adjusted by a mass flow controller (GF40 from BROOKS INSTRUMENT), cf. Figure 1, right. The gas tubing splits and is connected to the bubble column reactor held with marman clamps mounted on aluminium beams. The reactor is fitted with two half ring spargers (identical to the previous experiment) and two dip tube spargers ($d_o = 4\ mm$). At the bottom, a flexible rubber membrane is flanged between the base of the bubble column reactor and a flat ring. A high-performance slider (LinMot, PL01-20x240/180-HP) is connected to the membrane, located inside a linear motor (LinMot, PS01-37x120F-HP-C), which is linked to a controller and a computer (not shown). Experiments were performed at gas flow rates of 0.5 L/min, 1 L/min to 2.0 L/min.

Imaging apparatus

All images were recorded using a high-speed camera (FASTCAM, Mini AX50) and a LED panel light with a translucent optical diffuser layer (SRPL30x120, 11000 lux, 4000 K) that functions as a background illumination. The number of generated bubbles and their size vary both depending on the gas flow rate, sparger type, and sparger hole diameter. To compensate for these discrepancies, the frame rate and the total number of recorded frames are adjusted so that at least 2000 bubbles are evaluated for each case.

Image processing for bubble size and bubble generating frequency

Two different image processing algorithms are utilized: one for determining the bubble generating frequency (A) and another one for the bubble size (B). For both image processing algorithms, the pre-processing consists of: calculating an average background illumination

GALA e.V., Karlsruhe, Germany, ISBN 978-3-9816764-6-4

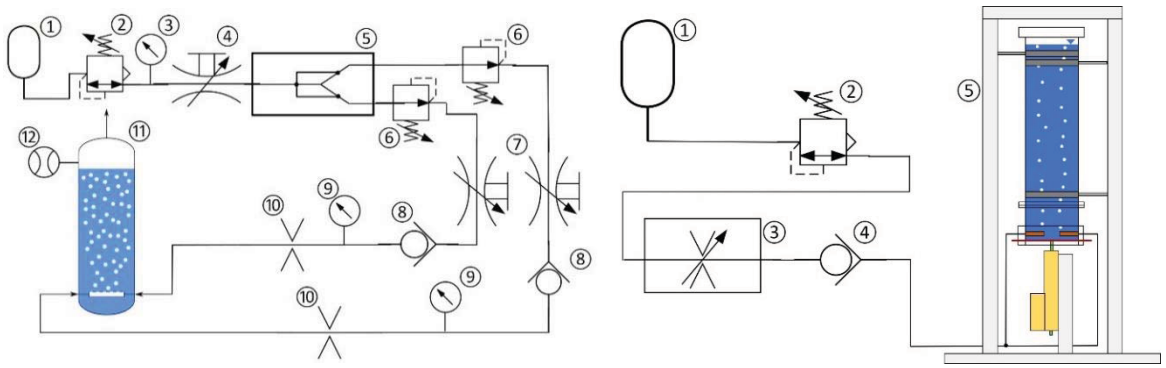

Figure 1 Left: air supply (1), pressure regulator (2), pressure gauge (3), throttle valve (4), fluidic oscillator (5), bleed valves (6), throttle valves (7), reflux valve (8), pressure gauge (9), restriction plate (10), bubble column reactor (11) and flow meter (12). Right: air supply (1), pressure regulator (2), mass flow controller (3), reflux valve (4), suspended bubble column reactor with linear motor (5)

(Bradley's method) and subtracting that image to isolate the bubbles from the background; increasing the contrast by remapping the intensity value distribution; and finally, the binarization of the image using Otsu's method for determine the binarization threshold.
(A) The bubble edges are detected by subtracting the dilated image from the eroded image, creating two clear edges of the bubble. This method proved to be a more reliable alternative to standard edge detection algorithms, such as Canny/Sobel edge detections. Afterwards, possible gaps in the object's edges are bridged and holes inside objects are filled. Then, all the white pixels in the bottom row of the image are summed and timestamped. From this time-dependent signal, the dominant frequency (bubble generating frequency) is extracted by applying the fast Fourier transformation.
(B) Because the measurement of the bubble size in dense bubble clouds is challenging, the image processing algorithm instead identifies and evaluates only isolated bubbles under the assumption, that every bubble size has the same probability to be overlaid (Ziegenhein et al., 2016). The classification of the overlaid bubbles is performed by identifying all regional maxima in the image (Figure 2, img 1), which corresponds to the bright spots in the centre of the bubbles (Figure 2, img 0). If more than one regional maxima is located inside an object, this object consists of more than one bubble and is discarded, cf. Figure 2 img 2 and 3.
Lastly, boundaries are set for the object's area and solidity (Area/ConvexArea) by a manual evaluation to exclude implausible detection caused by faulty background unification, coalesced bubbles from jetting, or other disturbances. Based on that, the equivalent circular area diameter is calculated.

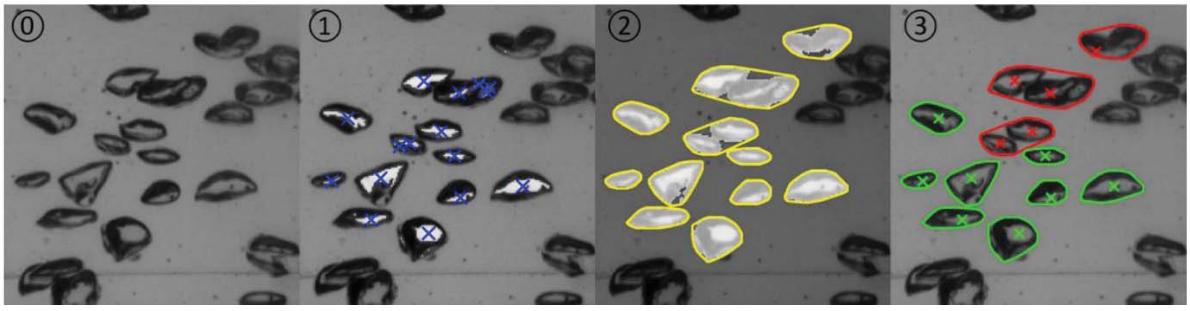

Figure 2 (0): The raw image is used as background image (ring sparger, gas flow rate of 0.8 L/min). (1): regional maxima are shown in white with blue crosses indicating their centroids. (2): From the binary image all identified objects (bubbles) are shown with their convex hulls. (3): The rejected bubbles are shown in red and accepted bubbles are shown green. Crosses indicate the centroid of the bubbles.

Audio analysis of the frequency of the fluidic oscillator

The frequency of the fluidic oscillator could be altered by changing the input gas flow rate and the length of the feed-back loop. The oscillating gas flow inside the fluidic oscillator creates an audible sound which was recorded with a microphone attached to the feed-back loop. From

GALA e.V., Karlsruhe, Germany, ISBN 978-3-9816764-6-4

the recorded audio signal, the oscillation frequency was extracted by using the fast Fourier transformation.

Gas hold-up

The gas hold-up is measured by using a pressure difference at two vertical position along the bubble column reactor. Two small transparent tubes are connected at these positions and positioned vertically. The water levels inside the small tubes (corresponding to the hydrostatic pressure inside the tubes) are recorded during operations of the bubble column reactor and the difference in height of the water level is evaluated over time. The gas hold-up is then calculated using the following equation

$$\varepsilon_g = \frac{\Delta h_1 - \Delta h_2}{\Delta h} \tag{1}$$

where $\Delta h_1$and Δh_2 are the change in water level before and during gas flow at the two positions and Δh is the height difference between the two positions of pressure measurement.

Results and Discussion

Oscillation of gas phase

Figure 3 shows the average bubble diameter for two dip tube spargers ($d_0 = 2\ mm$) as a function of the oscillation frequency, ranging from 150 Hz to 450 Hz, as a reference the average bubble diameter without oscillation (solid line) is chosen. As the gas flow rate increases, so does the average bubble diameter from approximately 6.3 mm, 8.75 mm, 9.6 mm to 10.4 mm, respectively. Predictions made by models and empirical correlation deviate from the experimental results less than 10 % for all flow rates (not shown) (Ramakrishnan et al. 1969, Wallis 1969). Over the full range of all oscillating frequencies, no clear trend for the average bubble diameter can be identified for any gas flow rates. To substantiate this observation, the analysis of variance by means of the Fisher's least significant difference procedure (F-LSD) is used to find significant differences (p = 5 %) between the reference bubble diameter and any other results, cf. Figure 3 (green square). Again, no clear trend can be detected as values seem to fluctuate randomly around an averaged value. To test this hypothesis, the average bubble

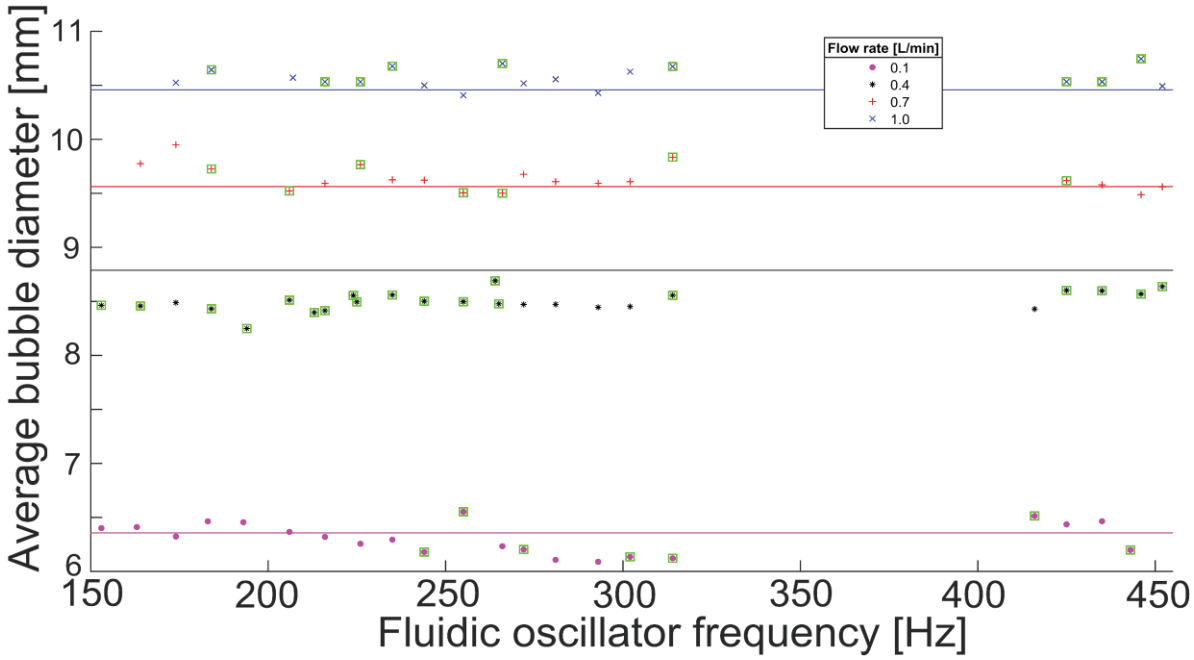

Figure 3 Average bubble diameter for one dip tube sparger ($d_0 = 2\ mm$) is plotted over the frequency of the fluidic oscillator for four different gas flow rates per sparger. The solid line indicates the average bubble diameter without an oscillation of the gas flow. Green squares mark the results that differ significantly (p = 5 %) from the reference.

GALA e.V., Karlsruhe, Germany, ISBN 978-3-9816764-6-4

diameter (d_b) is averaged for all oscillating frequencies (N) and the residuals (R) are calculated with the following equation:

$$R_i = d_{b,i} - \frac{\sum_{i=1}^{N} d_{b,i}}{N} \tag{2}$$

where $R_i$is the residual for the i-th oscillating frequency. If the residuals are normally distributed, then the effect of the oscillation of the gas flow is in fact caused by random fluctuations. The Anderson-Darling test and Kolmogorov-Smirnov test confirm that the residuals are in fact from a population with a normal distribution. This leads to the conclusion that under the tested conditions the oscillation of the gas phase does not significantly reduce the average bubble diameter.

For the bubble generating frequency (not shown), a very similar observation to the average bubble diameter was made: residuals (Equation 2) are also normally distributed around an oscillation averaged value, 8 Hz, 33 Hz, 35 Hz, to 38 Hz for the four gas flow rates, respectively. Analysis of the half ring sparger yielded that the average bubble diameter is unaffected by the oscillation frequency as well as gas flow rate. A manual evaluation of the video footage concluded that with an increasing the gas flow rate the bubble generating frequency at each sparger hole increased but the average bubble diameter remains constant (confirmed with image processing algorithm).

It is argued that the reduction in average bubble diameter is tied to precisely reaching an optimal oscillating frequency, at which a new bubble is created with each gas pulse (Brittle 2015). In this case, a lift force, associated with the momentum of the gas pulse entering the bubble, causes the bubble to detach prematurely. Exceeding the optimal oscillating frequency causes the momentum lift force to be insufficient to overcome the adhesive forces. On the other hand, below the optimal frequency, the pulse will be longer, therefore contain more gas, resulting in larger bubbles. Consequently, the bubble generating frequency and the optimal oscillating frequency must be equal and the momentum lift force needs to be large enough to have a significant impact the bubble detachment phase. In the conducted experiments the frequency ratio

$$f = \frac{\text{bubble generating frequency}}{\text{oscillating frequency}} \tag{3}$$

far exceeds the optimal value of unity and is closer to five, suggesting that this is the reason as to why no change in average bubble diameter could be experimentally detected. To further investigate this claim, a simulation of the bubble detachment phase was conducted at different

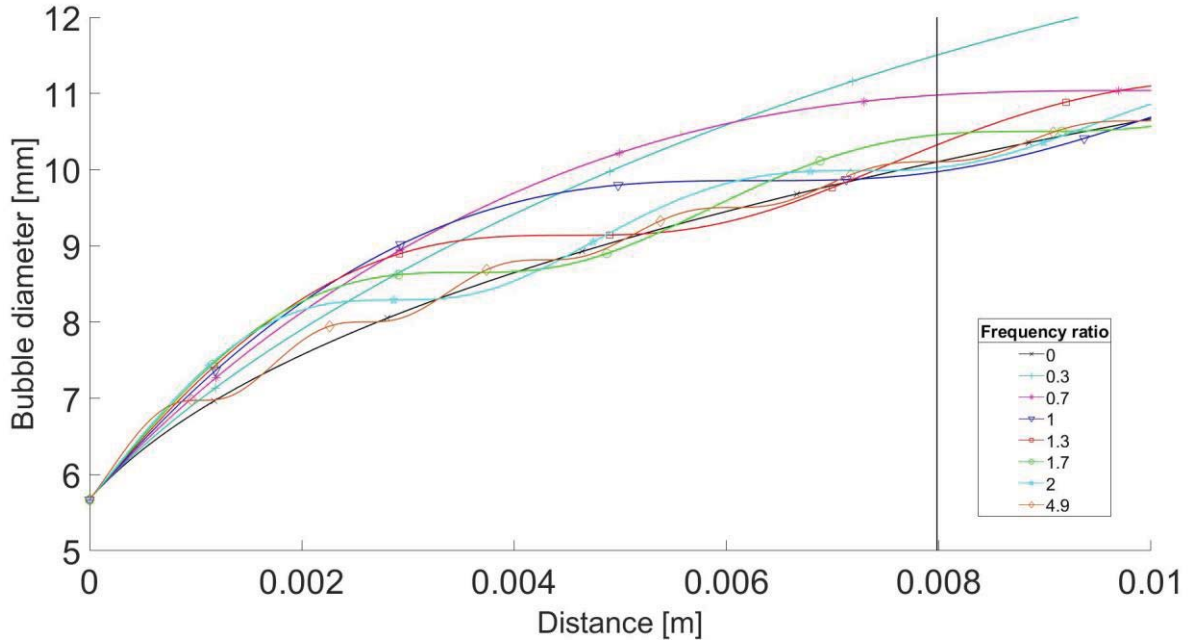

Figure 4 Simulated bubble diameter shown for different frequency ratios for a gas flow rate of 1.0 L/min as a function of the distance travelled by the bubble. The straight vertical line indicates the terminating condition.

GALA e.V., Karlsruhe, Germany, ISBN 978-3-9816764-6-4

frequency ratios. The bubble detachment was modelled with an equation of motion based on the two stage Ramakrishnan-Kumar-Kuloor model and Gaddis-Vogelpohl model (Ramakrishnan et al., 1969, Gaddis and Vogelpohl, 1986). The drag force due to expansion of the bubble volume is excluded. The time-dependent gas flow rate ($\dot{V}_t$) is approximated with a shifted sine wave function

$$\dot{V}_t = \dot{V}_c[\sin(2\pi\, f_{FO}\, t) + 1] \tag{4}$$

where $f_{FO}$is the oscillation frequency of the fluidic oscillator and $\dot{V}_c$ is the equivalent constant gas flow rate. As an initial condition for the bubble diameter, the analytic solution of the expansion phase is used based on the Ramakrishnan-Kumar-Kuloor model. As a terminating condition, a distance travelled by the bubble was used (three quarters of the bubbles length (Gaddis and Vogelpohl, 1986)). Deviations between simulated and measured bubble diameter are within five percent.

In Figure 4, the bubble diameter is shown as a function of the distance travelled by the bubble. The vertical line indicates the terminating condition. All oscillation frequencies, lower than the bubble generating frequency ($f < 1$), adversely influence the bubble diameter, with an increase of up to 20 % compared to the bubble diameter without gas oscillation. On the other hand, for frequency ratios far greater than unity, the bubble diameter is almost indistinguishable from the non-oscillating one.

Depending on the exact point of bubble detachment from the nozzle the frequency ratio should be either exactly unity or slightly greater for a bubble diameter reduction of up to 10 %.

Vibration of liquid phase

Figure 5 shows the normalized gas hold-up for a gas flow rate of 2 L/min (superficial gas velocity of 0.0087 m/s) as a function of the amplitude and frequency of vibration of the liquid phase for the dip tube sparger ($\mathrm{d}_0 = 4\ \mathrm{mm}$). As a normalization factor, the gas hold-up without any vibration of the liquid phase was used for the gas flow rate, so that an increase in gas hold-up can be solely contributed to the vibration of the liquid phase. A maximum increase in gas hold-up of 2.7 times was achieved by vibrating the liquid phase at a frequency of 25 Hz and an amplitude of 5 mm. It appears an amplitude above 3 mm increases the gas hold-up significantly. Similar trends were detected for lower gas flow rates of 0.5 and 1.0 L/min. Here, the relative maximum gas hold-up (1.7 times) occurred at the same frequency and amplitude (25 Hz and 5 mm) but their absolute values are smaller (40 % and 70% respectively). In case of

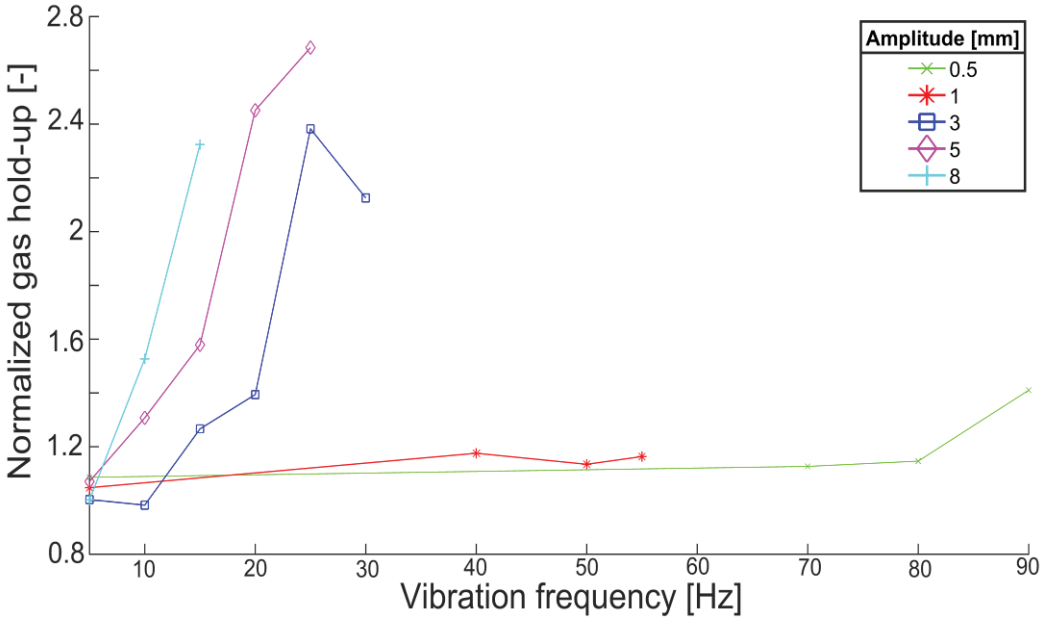

Figure 5 Normalized gas hold-up as a function of the frequency and amplitude of the liquid phase vibration using the dip tube sparger ($\mathrm{d}_0 = 4\ \mathrm{mm}$) for gas flow rates of 2.0 L/min with normalization factor (gas hold-up without the vibration of the liquid phase) of 0.0179.

GALA e.V., Karlsruhe, Germany, ISBN 978-3-9816764-6-4

the half ring sparger, vibrations had an overall stronger effect on the gas hold-up (approximately 35%, 67%, 92% for the three gas flow rates, respectively) than the dip tub sparger but the relative increase due to vibration is only approximately 70%. In combination with the required power input of the linear motor, an optimal combination of vibration amplitude and frequency and gas flow rates can be identified at 3 mm and 25 Hz with 2 L/min.

Bubble formation and bubble break-up

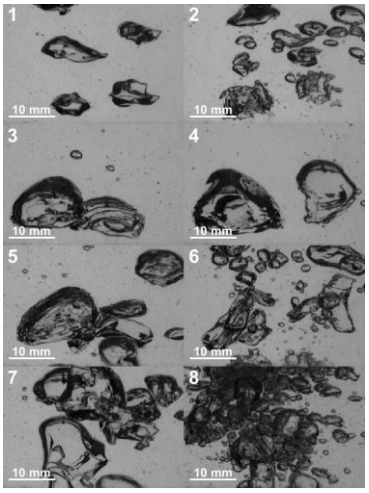

Figure 6 The gas flow rate for the first image series (images 1, 2) is 0.5 L/min and 2 L/min for all other image series (images 3, 4; 5, 6; and 7, 8). The frequencies and amplitudes are 15 Hz and 3 mm for the top two image series (images 2 and 4), 30 Hz and 3 mm for the third image series (image 5, 6), and 80 Hz and 1 mm for the last image series (images 7, 8).

Images are taken above the spargers and showing the bubble formation for different cases. The left images (uneven numbers) display the bubbles without vibration of the liquid phase and the right images (even numbers) with vibrations of the liquid phase. For the first two image series, the vibration conditions are identical (15 Hz and 3 mm) but the gas flow rate is increased from 0.5 to 2.0 L/min. The vibration of the liquid phase reduces bubble size by a factor of two and broadens the bubble size distribution (Image 1 and 2), with some bubbles approaching microbubble scale (< 1 mm). The bubble formation is also altered as the gas is propelled rapidly outwards of the sparger with every rising stroke of the linear motor. This effect is caused by high-velocity water 'suck-back' and gas explosions from the sparger (Knopf et al. 2006). But for a larger gas flow rate (Images 3 and 4), the energy input due to the vibration is insufficient to cause substantial bubble break-up (Image 4) to the larger bubbles. Doubling the vibration frequency (Images 5 and 6, 30 Hz and 3 mm), induces considerable bubble break-up (Image 6), which is also reflected in the doubling of the gas hold-up, cf. Figure 5. A further increase in power input (Images 7 and 8, 80 Hz and 1 mm) results in a dense bubble cloud that drastically increased the gas hold-up, where measurements become difficult to realize due to intense splashing at the top of the column. Results for the ring sparger were similar (not shown).

Figure 7 shows the bubble deformation further along the bubble column reactor that alters the bubble shape between a spherical shape and a flat, elliptic shape (at 90 Hz and 1 mm). The energy input is not large enough to cause the small bubbles break-up due to the forces caused by liquid oscillation. From extensive evaluation of video footage and simulations of a bubble

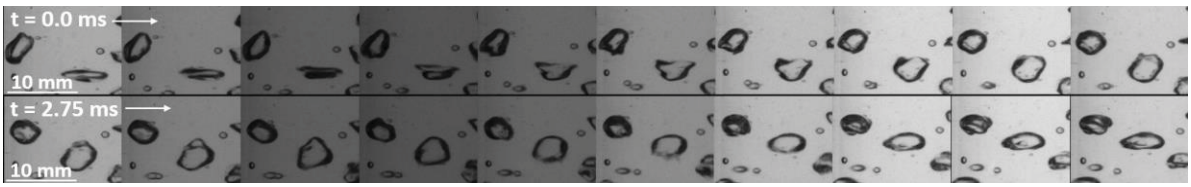

Figure 7 Image series shows the deformation of bubbles due to the vibration of the liquid phase for the ring sparger with gas flow rate of 2.0 L/min and vibration frequency and amplitude of 90 Hz and 1 mm. White arrows show the progress in time, the total time span is 5 ms.

GALA e.V., Karlsruhe, Germany, ISBN 978-3-9816764-6-4

(diameter of 4 mm) inside an oscillating box filled with water (Movassat el at. 2015), a critical Weber number ($\mathrm{We_c} = 1$) can be derived, at which bubble break-up begins to appear.

Conclusions

The experiments performed in this work focused on the characterization of bubble column reactors under the influence of forced pulsation of the gas and liquid phase. Quantitative measurements such as average bubble diameter, bubble generating frequency, and gas hold-up were conducted as well as qualitative observation classifying bubble formation, and bubble break-up. From that, the following conclusions can be drawn:

- For ratios of the gas oscillation frequency and bubble generating frequency greater than approximately five, no statistically significant reduction of the average bubble diameter is possible for either dip tube or ring sparger, cf. Figure 3.
- In computer simulation, if the gas oscillation frequency was set slightly higher than the bubble generating frequency, a bubble diameter reduction of 10 % could be achieved for a gas flow rate of 1.0 L/min cf. Figure 4, similar as reported by (Brittle et al., 2015).
- Vibration of the liquid phase can further increase the gas hold-up up to 2.8 times for the dip tube sparger and 1.8 times for the ring sparger, cf. Figure 5.
- Bubble break-up mostly occurs inside or in the vicinity of the sparger under liquid oscillating conditions, while almost no bubble breakage was detected further up the column, cf. Figure 7
- Gas flow rate, sparger type, and bubble diameter specific energy thresholds exist after which bubble break-up is only possible, cf. Figure 6, Images 4 and 6.

Literature

Mahmood K. H. Al-Mashhadani, H. C. Hemaka Bandulasena, and William B. Zimmeman. “CO2 Mass Transfer Induced through an Airlift Loop by a Microbubble Cloud Generated by Fluidic Oscillation”. In: Industrial & Engineering Chemistry Research 51.4 (2011)

Mahmood K.H. AL-Mashhadani, Stephen J. Wilkinson, and William B. Zimmerman. “Airlift bioreactor for biological applications with microbubble mediated transport processes”. In: Chemical Engineering Science 137 (2015), pp. 243–253.

M.H.I. Baird and J.F. Davidson. “Gas absorption by large rising bubbles”. In: Chemical Engineering Science 17.2 (1962), pp. 87–93.

Stuart Brittle et al. “Minimising microbubble size through oscillation frequency control”. In: Chemical Engineering Research and Design 104 (2015), pp. 357–366.

J. Ellenberger, J.M. van Baten, and R. Krishna. “Intensification of bubble columns by vibration excitement”. In: Catalysis Today 79-80 (2003), pp. 181–188.

E.S. Gaddis and A. Vogelpohl. “Bubble formation in quiescent liquids under constant flow conditions”. In: Chemical Engineering Science 41.1 (1986), pp. 97–105

K. L. Harbaum and G. Houghton. “Effects of sonic vibrations on the rate of absorption of carbon dioxide in gas bubble-beds”. In: Journal of Applied Chemistry 12.5 (1962), pp. 234–240.

F. Carl Knopf et al. “Pulsing to improve bubble column performance: I. Low gas rates”. In: AIChE Journal 52.3 (2006), pp. 1103–1115.

Rajamani Krishna and J Ellenberger. “Improving Gas–liquid Contacting in Bubble Columns by Vibration Excitement”. In: International Journal of Multiphase Flow 28.7 (July 2002), pp. 1223–1234

S. Ramakrishnan, R. Kumar, and N.R. Kuloor. “Studies in bubble formation—I bubble formation under constant flow conditions”. In: Chemical Engineering Science 24.4 (1969), pp. 731–747.

Mohammad Movassat, Nasser Ashgriz, and Markus Bussmann. “Oscillation and breakup of a bubble under forced vibration”. In: International Journal of Heat and Fluid Flow 54 (2015), pp. 211–219.

Vaclav Tesar, Chuan-Hsiang Hung, and William B. Zimmerman. “No-moving-part hybrid-synthetic jet actuator”. In: Sensors and Actuators A: Physical 125.2 (2006), pp. 159–169.

Y. G. Waghmare, F. Carl Knopf, and Richard G. Rice. “The Bjerknes effect: Explaining pulsed-flow behavior in bubble columns”. In: AIChE Journal 53.7 (2007), pp. 1678–1686.

Graham B. Wallis. One Dimensional Two-Phase Flow. McGraw-Hill, 1969. ISBN: 978-0070679429.

T. Ziegenhein et al. “On the hydrodynamics of airlift reactors, Part I: Experiments”. In: Chemical Engineering Science 150 (2016), pp. 54–65.

GALA e.V., Karlsruhe, Germany, ISBN 978-3-9816764-6-4